Galpha13 stimulates cell migration through cortactin-interacting protein Hax-1.

Venkat Radhika, Djamila D. Onesime, Ji Hee Ha, N. Dhanasekaran

THE JOURNAL OF BIOLOGICAL CHEMISTRY
Vol. 279, No. 47, Issue of November 19, pp. 49406–49413, 2004
Printed in U.S.A.

$G\alpha_{13}$ Stimulates Cell Migration through Cortactin-interacting Protein Hax-1*

Received for publication, August 3, 2004
Published, JBC Papers in Press, August 31, 2004, DOI 10.1074/jbc.M408836200

V. Radhika‡, Djamila Onesime‡§, Ji Hee Ha‡, and N. Dhanasekaran¶

From the Fels Institute for Cancer Research and Molecular Biology, Temple University School of Medicine, Philadelphia, Pennsylvania 19140

$G\alpha_{13}$, the α-subunit of the heterotrimeric G protein G13, has been shown to stimulate cell migration in addition to inducing oncogenic transformation. *Cta*, a *Drosophila* ortholog of G13, has been shown to be critical for cell migration leading to the ventral furrow formation in *Drosophila* embryos. Loss of $G\alpha_{13}$ has been shown to disrupt cell migration associated with angiogenesis in developing mouse embryos. Whereas these observations point to the vital role of G13-orthologs in regulating cell migration, widely across the species barrier, the mechanism by which $G\alpha_{13}$ couples to cytoskeleton and cell migration is largely unknown. Here we show that $G\alpha_{13}$ physically interacts with Hax-1, a cytoskeleton-associated, cortactin-interacting intracellular protein, and this interaction is required for $G\alpha_{13}$-stimulated cell migration. Hax-1 interaction is specific to $G\alpha_{13}$, and this interaction is more pronounced with the mutationally or functionally activated form of $G\alpha_{13}$ as compared with the wild-type $G\alpha_{13}$. Expression of Hax-1 reduces the formation of actin stress fibers and focal adhesion complexes in $G\alpha_{13}$-expressing NIH3T3 cells. Coexpression of Hax-1 also attenuates $G\alpha_{13}$-stimulated activity of Rho while potentiating $G\alpha_{13}$-stimulated activity of Rac. The presence of a quadnary complex consisting of $G\alpha_{13}$, Hax-1, Rac, and cortactin indicates the role of Hax-1 in tethering $G\alpha_{13}$ to the cytoskeletal component(s) involved in cell movement. Whereas the expression of Hax-1 potentiates $G\alpha_{13}$-mediated cell movement, silencing of endogenous Hax-1 with Hax-1-specific small interfering RNAs drastically reduces $G\alpha_{13}$-mediated cell migration. These findings, along with the observation that Hax-1 is overexpressed in metastatic tumors and tumor cell lines, suggest a novel role for the association of oncogenic $G\alpha_{13}$ and Hax-1 in tumor metastasis.

Cell migration plays a vital role in different biological processes ranging from embryogenesis to immune response (1, 2). However, an aberrant activation of cell migration in neoplastic cells results in tumor metastasis. Cells migrate in response to different cues through the coordinated interactions of actin- and/or microtubule-associated cytoskeletal proteins (3, 4). G protein-coupled receptors and their cognate G proteins play a major role in regulating cell migration and chemokinesis (5). The G12 family of G proteins, defined by α-subunits $G\alpha_{12}$ and $G\alpha_{13}$, has been shown to activate novel signaling pathways involved in cell growth and neoplastic transformation (6). Two lines of evidence indicate that the α-subunit of G13, $G\alpha_{13}$, is primarily involved in the regulation of cell migration (7–9). The first is the observation that *Cta*, an ortholog of $G\alpha_{13}$, is critically required for cell movement during *Drosophila* embryogenesis (7). The second is the finding that $G\alpha_{13}$-null ($G\alpha_{13}-/-$) fibroblasts show the loss of chemokinetic response to thrombin or lysophosphatidic acid receptor-mediated cell movement (8, 9).

Existing models of cell movement suggest that the initial movements in cell migration involve polymerization of filamentous actin at the leading edge forming membrane extensions (3, 4). Subsequent adhesion at the leading edge is followed by the translocation of the cell body by the forward flow of the cytosol. Finally, whereas the leading edge of the cell is still attached to the substratum, the rear-end is detached and retracted into the cell body thereby effecting cell movement. All of these distinct phases of cell movement, with the exception of cytosolic translocation, involve temporal and spatial regulation of actin polymerization and depolymerization. Although, many different proteins control actin polymerization, several lines of evidence indicate that the interaction between cortactin and actin-related proteins 2/3 plays a critical role in actin polymerization leading to cell movement (10–12). Cortactin is a major substrate for tyrosine kinases such as Src, Fer, and Syk, and is usually present in the cytosol. Upon growth factor stimulation, it is translocated by activated Rac-1 to cell periphery where it interacts with F-actin and stimulates actin-related protein 2/3-mediated actin polymerization (13). As a result, tyrosine kinases as well as small GTPases converge on cortactin to stimulate actin polymerization and consequent cell movement. Although $G\alpha_{13}$ has been known to be involved in the regulation of thrombin and lysophosphatidic acid-receptor-stimulated cell migration of fibroblasts (8, 9), the mechanism by which $G\alpha_{13}$ stimulates cell movement or the identity of the signaling components involved in $G\alpha_{13}$-mediated cytokinesis is largely unknown. Therefore, we sought to identify the signaling components involved in $G\alpha_{13}$-mediated cell movement. Here we demonstrate that $G\alpha_{13}$ physically associates with intracellular protein Hax-1, which has been previously identified as a cortactin-interacting protein (14) and that Hax-1 promotes $G\alpha_{13}$-mediated cell migration. Furthermore, we show that $G\alpha_{13}$ and Hax-1 exists in a complex consisting of Rac and cortactin. We also demonstrate that the coexpression of Hax-1 enhances $G\alpha_{13}$-mediated Rac activity while inhibiting Rho activity, both of which can promote cell movement. These results describe for the first time a critical role for Hax-1 in cell movement mediated by $G\alpha_{13}$.

* This work was supported by National Institutes of Health Grant GM49897. The costs of publication of this article were defrayed in part by the payment of page charges. This article must therefore be hereby marked "*advertisement*" in accordance with 18 U.S.C. Section 1734 solely to indicate this fact.

‡ These authors made equal contributions to this study.

§ Present address: Laboratoire de Génétique Moléculaire et Cellulaire Institut National de la Recherche Agrnomique-Centre National de la Recherche Scientifique, Institut National Agronomique Paris-grignon, F-78850 Thiverval-Grignon, France.

¶ To whom correspondence should be addressed. Tel.: 215-707-1941; Fax: 215-707-5963; E-mail: danny001@temple.edu.

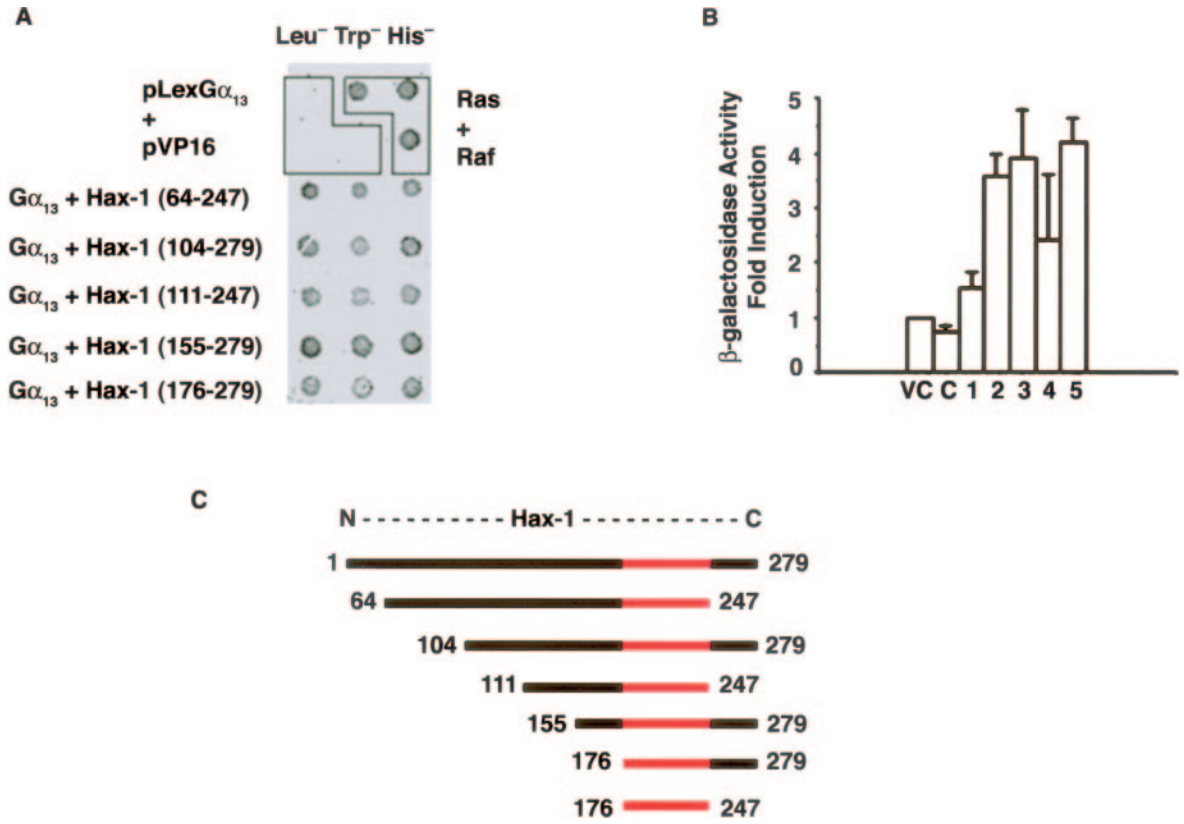

FIG. 1. **Two-hybrid assays for the interaction of Gα_{13} with Hax-1.** *A*, interaction of Gα_{13} and Hax-1 in yeast cells. Diploids showing Gα_{13}-Hax-1 interactions were first selected on synthetic medium lacking Leu and Trp, and the replicate colonies were tested for their ability to grow on medium lacking Leu, Trp, and His. L40 yeast cells expressing pLex-Ras plus pGAD-GH-Raf as indicated by the triplicate colonies labeled Ras + Raf, were used as controls for positive interaction. Yeast cells expressing pLEXGα_{13}-ED plus vector pVP16 as indicated by the triplicate colonies labeled pLexGα_{13} + pVP16, were used as negative control to show the absence of interaction. *B*, β-galactosidase assay validating Gα_{13}-Hax-1 interactions. Diploids were grown on minimal medium and were measured using *o*-nitrophenyl β-D-galactopyranoside as substrate. *VC*, vector control; *C*, Gα_{13} + pVP16; *1*, Gα_{13} + Hax-1-(64–247); *2*, Gα_{13} + Hax-1-(104–279); *3*, Gα_{13} + Hax-1-(111–247); *4*, Gα_{13} + Hax-1-(155–279); and *5*, Gα_{13} + Hax-1-(176–247); the activity is presented as -fold change over the vector control values that were taken as 1. *C*, delineating the Hax-1 core domain involved in the Gα_{13} interaction. Using the sequences derived from different Gα_{13}-interacting Hax-1 inserts, the core domain of Hax-1 involved in Gα_{13} interaction is defined.

EXPERIMENTAL PROCEDURES

Plasmids, Strains, and Cells—The yeast expression vector pLexA-Gα_{13}ED was constructed by ligating the PCR-derived cDNA insert encoding amino acids 221–347 of Gα_{13} into pBTM116 vector. Expression vector pcDNA3-Hax-1 was constructed by ligating the EcoRI-SpeI-excised Hax-1 insert from pME18S-Hax-1 into the EcoRI and XbaI site of pcDNA3 vector. C-terminal S-protein-tagged Hax-1 was constructed by replacing the stop codon of Hax-1 with the coding sequence for the S-tag (KETAAAKFERQHMDS) followed by a stop codon. The resultant Hax-1-S-tag was cloned into the pcDNA3 vector. Cell lines Gα_{13}QL- and Gα_{13}WT-NIH3T3 have been previously described (31). All the constructs were verified by sequencing. Transfection of NIH3T3 cells was carried out using the calcium phosphate method as previously described (32). COS-7 cells were transfected using FuGENE-6 reagent (Roche Applied Science) according to the manufacturer's protocol.

Yeast Two-hybrid Screen—The yeast two-hybrid screen was performed in yeast strain L40 transformed with pLexA-Gα_{13}ED and plasmid pGAD-GH containing an oligo(dT)-primed HeLa cell cDNA library (Clontech, Palo Alto, CA). Of the 4×10^6 transformants screened, 550 clones were found to grow in the absence of His. The His+ colonies were restreaked on SD−His/−Leu/−Trp plates and subjected to β-galactosidase activity using a filter assay. The resultant 454 His+Lacz+ colonies were grown in SD-Leu medium to enable the segregation of pLexA-Gα_{13}ED. The Trp-Leu+ segregates were mated to yeast strain AMR70 that had been pre-transformed with the plasmid pLex-Lamin or pLexA-Gα_{13}ED. The leu+ trp+ diploids were then assayed for transactivation of the lacZ reporter by a filter assay. The positive clones totaling 115 that showed β-galactosidase activity only in the presence of pLexA-Gα_{13}ED were isolated and the library plasmids were recovered. The cDNA inserts of the library plasmids were amplified by PCR and 10 representative clones were further sequenced. The sequence analysis of the cDNA inserts revealed that they are five independent fusions of human Hax-1.

Co-precipitation and Immunoblot Analysis—Co-precipitation studies were carried out with COS-7 cells using S-protein-agarose (Novagen, EMD Biosciences, Inc., Madison, WI) or antibodies specific to the protein of interest. At 24 h following transfection, cells were lysed and cell lysate protein (1 μg each) was incubated with 35 μl of S-protein-agarose for 4 h at 4 °C. After repeated washes with lysis buffer, the S-protein-agarose-bound proteins were separated by SDS-PAGE and electroblotted onto polyvinylidene difluoride membranes. Co-immunoprecipitation analyses were carried out by incubating cell lysate protein (1 μg each) with 1–5 μg of the respective antibodies for 4 h at 4 °C followed by the addition of 30 μl of 50% slurry of protein A-Sepharose (Amersham Biosciences). Antibodies to cortactin (05-180) and Rac (05-389) were from Upstate Signaling Solutions (Charlottesville, VA), whereas antibodies to the hemagglutinin epitope (2362) and Hax-1 (H65220) were from Cell Signaling (Beverly, MA), and BD Biosciences (San Jose, CA) respectively. Antibodies to S-epitope (SC-802), Gα_s (sc-823), Gα_q (sc-393), and Gα_{12} (sc-409) were from Santa Cruz Biotechnology Inc. (Santa Cruz, CA). Antibodies to Gα_i (1521) were a kind gift from Dr. David Manning, University of Pennsylvania, Philadelphia, PA. For immunoblot and immunoprecipitation studies for Gα_{13}WT and Gα_{13}QL, rabbit polyclonal antibodies (AS1-89-2) raised against the C terminus of Gα_{13} were used. After washing the immunoprecipitates twice with lysis buffer, the immunoprecipitated proteins were separated by SDS-PAGE and electroblotted onto polyvinylidene difluoride membranes. Immunoblot analyses with specific antibodies were carried out following the previously published procedures (31).

Co-localization of Hax-1 and Gα_{13}—Cells were grown on coverslips for 48 h, fixed with 3% paraformaldehyde in PBS[1] for 10 min, perme-

[1] The abbreviations used are: PBS, phosphate-buffered saline; siRNA, short interfering RNA; WT, wild-type.

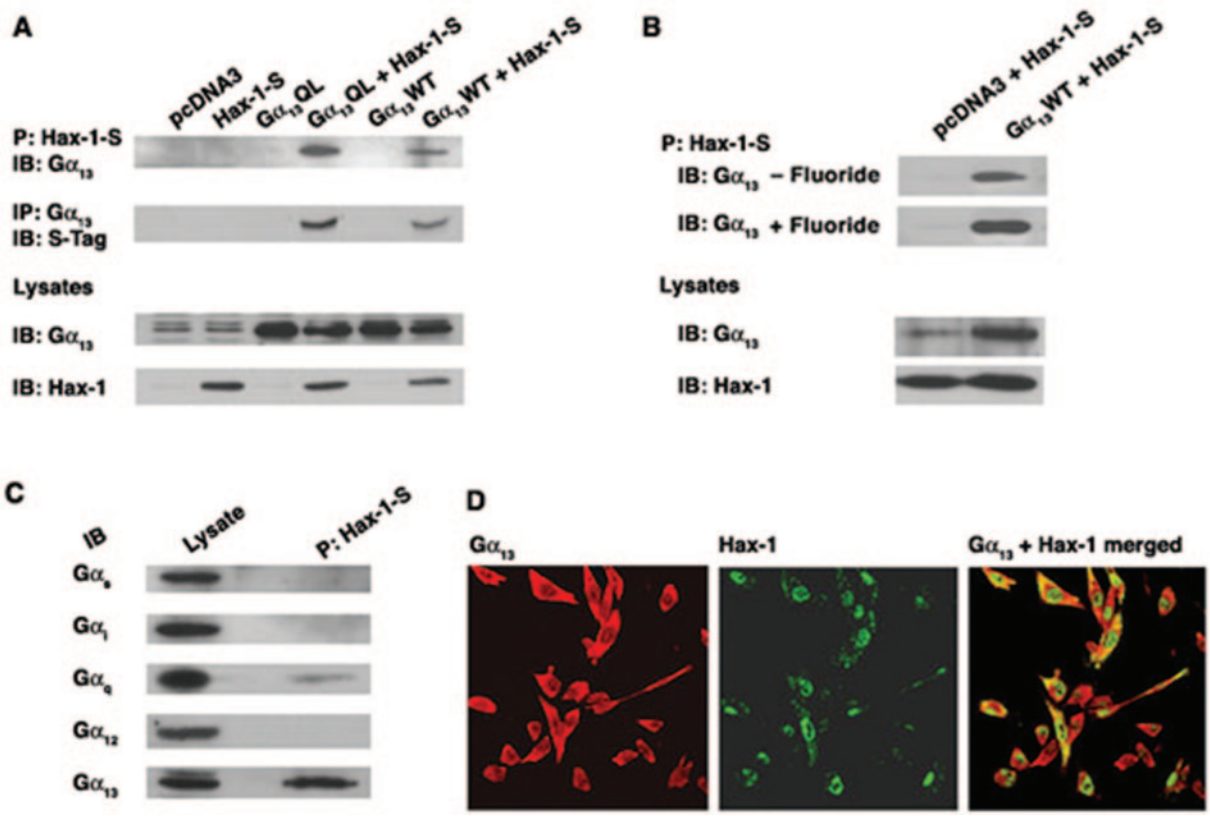

FIG. 2. **Association of $G\alpha_{13}$ with Hax-1.** *A*, interaction of $G\alpha_{13}$ and Hax-1 in COS-7 cells. COS-7 cells were transfected with pCDNA3 constructs encoding activated mutant ($G\alpha_{13}QL$) or wild-type ($G\alpha_{13}WT$) along with S-tagged Hax-1 (*Hax-1-S*) for 24 h. $G\alpha_{13}$ was co-precipitated with S-protein-agarose (*upper panel*), whereas Hax-1 was co-immunoprecipitated (*IP*) with anti-$G\alpha_{13}$ antibodies (*lower panel*). Expression of the transfected $G\alpha_{13}WT$, $G\alpha_{13}QL$, and Hax-1 were monitored by immunoblot (*IB*) analyses of the cell lysates (*panel under Lysates*) with the respective antibodies. *B*, effect of aluminum fluoride-stimulated activation of $G\alpha_{13}$ on Hax-1 interaction. COS-7 cells were co-transfected with a vector encoding epitope-tagged Hax-1 along with $G\alpha_{13}WT$ (*Hax-1 + $G\alpha_{13}WT$*) or vector control (*pcNA3 + Hax-1*) for 24 h. The transfectants were preincubated with 10 mM $AlCl_3$ plus 10 mM NaF for 15 min (*+Fluoride*) prior to lysis along with the non-treated control group (*−Fluoride*). $G\alpha_{13}$ subunits co-precipitated along with Hax-1 by S-protein-agarose (*P: Hax-1-S*) were identified by immunoblot analysis using $G\alpha_{13}$ antibodies (*upper panel*). Expression levels of Hax-1 and $G\alpha_{13}$ in these transfectants were monitored by immunoblot analyses with respective antibodies (*lower panel*). *C*, specificity of $G\alpha_{13}$-Hax-1 interaction. COS-7 cells were transfected with pCDNA3 constructs encoding activated mutants of $G\alpha_s$ ($G\alpha_sQL$), $G\alpha_i$ ($G\alpha_iQL$), $G\alpha_q$ ($G\alpha_qQL$), $G\alpha_{12}$ ($G\alpha_{12}QL$), and $G\alpha_{13}$ ($G\alpha_{13}QL$) along with S-tagged Hax-1 (*Hax-1-S*) for 24 h. $G\alpha$ subunits that were co-precipitated along with Hax-1-S by S-protein-agarose were identified by immunoblotting with the antibodies to the respective $G\alpha$-subunits as indicated. The expression levels of these subunits in the lysates were monitored for comparison (*under panel labeled lysate*). *D*, colocalization of $G\alpha_{13}$ and Hax-1. NIH3T3 cells stably expressing $G\alpha_{13}QL$ were transiently transfected with vectors encoding Hax-1 for 48 h. The cells were immunostained with antibodies to $G\alpha_{13}$ followed by Texas Red-labeled anti-rabbit IgG (*red*) for the expression of $G\alpha_{13}$ and antibodies to Hax-1 followed by Alexa 488-labeled anti-mouse IgG (*green*) for the expression of Hax-1. Colocalization of $G\alpha_{13}$ and Hax-1 is shown by dual channel imaging of red and green channels (*yellow*). These results are representative of triplicate experiments. The *scale bar* (*20 μm*) is common to all.

ablized by 0.05% Triton X-100 (10 min), blocked with 1% bovine serum albumin in PBS (30 min), and incubated with mouse monoclonal antibodies to Hax-1 or rabbit polyclonal antibodies to $G\alpha_{13}$ (1:200) for 1 h at 25 °C. After washing, samples were incubated with 1:100 dilution of Alexa Fluor 488-labeled goat anti-mouse IgG or Texas Red-labeled goat anti-rabbit IgG (Molecular Probes, Eugene, OR) for 1 h at 25 °C to obtain immunofluorescent imaging of Hax-1 and $G\alpha_{13}$, respectively. The coverslips containing the cells were washed with PBS, which were mounted on glass slides with 10 μl of Prolong Antifade reagent (Molecular Probes, Eugene, OR). The images were recorded and analyzed using an Olympus confocal microscope with a ×60/NA 1.4 plan-apochromat objective.

Actin Staining—Actin staining was carried out using fluorescein isothiocyanate-labeled phalloidin (Sigma) following previously published methods (33). Briefly, NIH3T3 cells/transfectants of interest were fixed on coverslips with 3% formaldehyde. After washing with PBS the cells were incubated at 37 °C in PBS containing 1 μM fluorescein isothiocyanate-phalloidin, 0.01% lysolecithin, and 0.05% bovine serum albumin for 10 min. At the end of the incubation, the cells were washed with PBS containing 2% bovine serum albumin and examined under a fluorescent microscope.

Cell Migration Assay—Cell migration assay was carried out in cell culture inserts (PET membrane with 8-μm pores, BD Biosciences). The cell culture inserts containing 3×10^4 cells in 200 μl of serum-free Dulbecco's modified Eagle's medium was placed in the well of the companion plate containing 500 μl of Dulbecco's modified Eagle's medium with 5% serum per well. Cells were incubated at 37 °C for 3 h. Non-migrating cells on the inner side of the inserts were removed with a cotton swab and the migrated cells on the underside of the insert were fixed and stained with Hemacolor (EMD Chemicals Inc., Gibbstown, NJ). Photomicrographs of three random fields were taken and enumerated to calculate the average number of cells that had migrated.

Silencing Hax-1 with Short Interfering RNAs (siRNA)—siRNA targeting mouse Hax-1, coding regions 188–208 bases (5′-AATTCGGTTTCAGCTTCAGCC-3′), was synthesized and purified (Qiagen Inc., Valencia, CA). An equimolar pool containing four different nonspecific control siRNA duplexes (number D-0011206-13-05, Dharmacon, Inc., Lafayette, CO) were used as control. Cells were transfected with 20 μM siRNA at 24-h intervals using TransMessenger reagent (Qiagen Inc.) for 96 h.

Rac/Rho Activation Assay—NIH3T3 cells stably expressing $G\alpha_{13}WT$ or $G\alpha_{13}QL$ were transiently transfected with pCDNA3-Hax-1. At 48 h following transfection, cells were lysed and the Rho or Rac pull-down assay was carried out according to the manufacturer's protocol (Upstate Signaling Solutions, Charlottesville, VA). Activated GTP-bound Rho was pulled-down from 1 mg of lysate protein using 20 μg of Rhotekin-RBD-(7–89)-agarose beads. The pulled-down Rho was identified by immunoblot analysis using anti-Rho (-A, -B, and -C). Active GTP-bound Rac was assayed by pulling down active Rac using 10 μg of PAK-PBD-(67–150)-agarose beads from 1 mg of lysates. The pulled-down Rac-GTP was identified by immunoblot analysis using anti-Rac antibody.

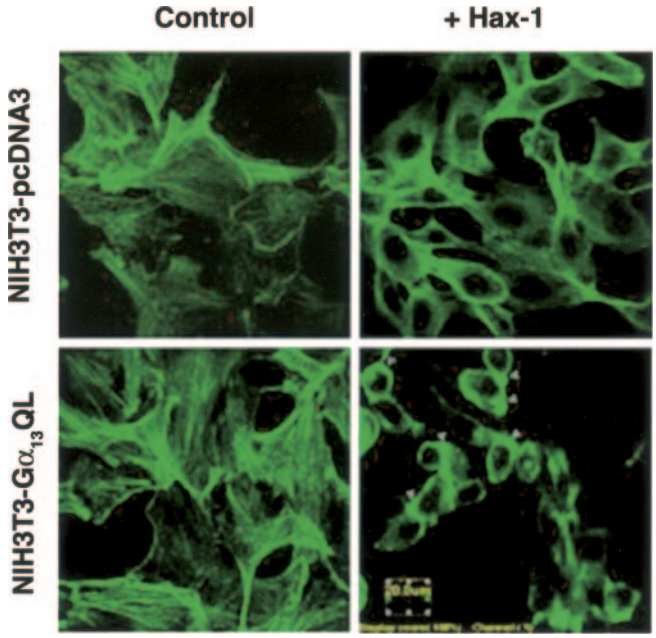

FIG. 3. **Reduction of stress fibers by Hax-1.** NIH3T3 cells stably expressing the empty vector (*NIH3T3-pcDNA3*) or $G\alpha_{13}$QL (*NIH3T3-$G\alpha_{13}$QL*) were transiently transfected with pcDNA3-Hax-1. At 48 h following transfection, the transfectants were stained for actin using fluorescein isothiocyanate-phalloidin and fluorescent imaging was carried out under a fluorescent microscope (*Scale bar*, 20 μm). Photomicrographs compare the effect of Hax-1 expression on actin stress fibers (*right panel*) in NIH3T3 cells expressing NIH3T3-pcDNA3 or NIH3T3-$G\alpha_{13}$QL cells (*left panel*). Three independent experiments yielded similar results and the results of a representative experiment are shown.

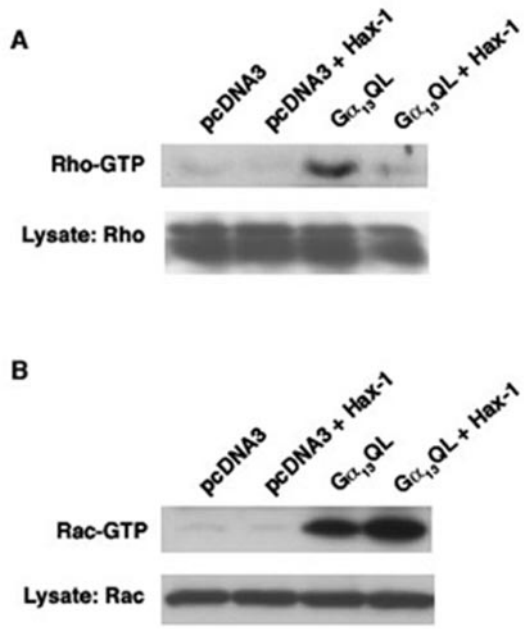

FIG. 4. **Hax-1 modulation of $G\alpha_{13}$-mediated activities of Rho GTPases.** *A*, activation of Rho by $G\alpha_{13}$ is attenuated by Hax-1. NIH3T3 cells stable expressing empty vector or $G\alpha_{13}$QL were cotransfected with vector encoding Hax-1. At 48 h after transfection, the cells were lysed and the lysates were incubated with Rhotekin-RBD-(7–89)-agarose beads (20 μg) at 4 °C for 45 min. The beads were washed, and bound Rho-GTP was detected by immunoblot analysis using polyclonal antibodies that recognize Rho-A, -B, and -C (*upper panel*). Immunoblot analysis of Rho in the cell lysate is presented for comparison (*lower panel*). *B*, activation of Rac by $G\alpha_{13}$ is attenuated by Hax-1. NIH3T3 cells stablely expressing empty vector or $G\alpha_{13}$QL were co-transfected with pcDNA3 vector encoding Hax-1. At 48 h after transfection, the cells were lysed and cell lysates were incubated with PAK-PBD-(67–150)-agarose beads (10 μg) at 4 °C for 45 min. The beads were washed, and bound Rac-GTP was detected by immunoblot analysis using polyclonal antibodies to Rac (*upper panel*). Immunoblot analysis of Rac in the cell lysate is presented for comparison (*lower panel*).

RESULTS

Interaction of $G\alpha_{13}$ with Hax-1—To identify novel signaling proteins that interact with $G\alpha_{13}$, a yeast two-hybrid screen was carried out in which the effector interacting domain of $G\alpha_{13}$ spanning amino acids 221–347, deduced from the crystal structures of the $G\alpha_t$ and $G\alpha_I$ (15), was used as bait in a human HeLa cell cDNA library. Analyses of a set of transformants that were positive for $G\alpha_{13}$ interaction identified Hax-1 (HS-1 associated protein X-1) as a $G\alpha_{13}$-interacting protein. Previous studies have identified Hax-1 as an intracellular, 35-kDa HS-1 or cortactin-interacting protein (14, 16). Sequence analyses of Hax-1 inserts rescued from these transformants revealed that Hax-1 coding sequences of varying lengths interact with $G\alpha_{13}$ (Fig. 1*A*). The interactions between these Hax-1 inserts and $G\alpha_{13}$ were also verified using β-galactosidase activity of the LacZ reporter gene (Fig. 1*B*). Sequence alignment of the different $G\alpha_{13}$-interacting Hax-1 fragments indicated that amino acids 176–247 of Hax-1 was sufficient for its interaction with $G\alpha_{13}$ (Fig. 1*C*).

To examine the *in vivo* interaction between $G\alpha_{13}$ and Hax-1, co-immunoprecipitation studies were carried out in COS-7 cells that were cotransfected with an expression vector containing a cDNA insert encoding S-epitope-tagged Hax-1 and a vector containing an insert encoding wild-type $G\alpha_{13}$ ($G\alpha_{13}$WT) or its activated mutant ($G\alpha_{13}$QL). Examination of $G\alpha_{13}$ immunoprecipitates for the presence of Hax-1 indicated that Hax-1 was coimmunoprecipitated with $G\alpha_{13}$ (Fig. 2*A*). Similarly, examination of Hax-1 immunoprecipitates by immunoblot analysis showed that $G\alpha_{13}$ was coimmunoprecipitated with Hax-1, thereby confirming the physical interaction between these two proteins. Although both $G\alpha_{13}$WT and its activated mutant $G\alpha_{13}$QL could be seen to interact with Hax-1, the interaction between $G\alpha_{13}$QL and Hax-1 is more pronounced than that of the wild-type (Fig. 2*A*). Furthermore, pretreatment of $G\alpha_{13}$WT transfectants with aluminum fluoride for 15 min, which is known to convert the unstimulated wild-type α-subunit to an active conformation (17, 18), drastically enhanced the interaction of Hax-1 with $G\alpha_{13}$WT, demonstrating that the active configuration of $G\alpha_{13}$ more avidly interacts with Hax-1 (Fig. 2*B*). Co-immunoprecipitation analyses to investigate whether Hax-1 interacts with the α-subunits of other G proteins subfamilies represented by $G\alpha_s$, $G\alpha_i$, and $G\alpha_q$, indicated that Hax-1 failed to interact with any of these α-subunits (Fig. 2*C*). Interestingly, a similar analysis to determine the interaction between Hax-1 and $G\alpha_{12}$, the α-subunit closely related to $G\alpha_{13}$, indicated that Hax-1 does not interact with $G\alpha_{12}$ thereby indicating the specificity of $G\alpha_{13}$-Hax-1 interaction (Fig. 2*C*). These results are significant in light of the observations that only $G\alpha_{13}$, but not $G\alpha_{12}$, is involved in the cell migratory response (9). The interaction between $G\alpha_{13}$ and Hax-1 can also be observed in NIH3T3 cells stably expressing $G\alpha_{13}$QL in which Hax-1 is transiently expressed. Double immunofluorescent labeling of $G\alpha_{13}$ and Hax-1 followed by image-merging analysis indicated the colocalization of $G\alpha_{13}$ and Hax-1 in NIH3T3 cells, further confirming their interaction in a cell-type independent manner (Fig. 2*D*). These findings, taken together with the previous observations, that $G\alpha_{13}$ regulates cell migratory response (8, 9) and Hax-1 interacts with cortactin (16), which promotes cell migration (10–13), suggested to us the interesting possibility that Hax-1 is involved in linking $G\alpha_{13}$ to cell migration-associated actin cytoskeletal motor.

Cytoskeletal Changes in $G\alpha_{13}$-Hax-1 Co-transfectants—Previous studies from others, as well as us, have also shown that

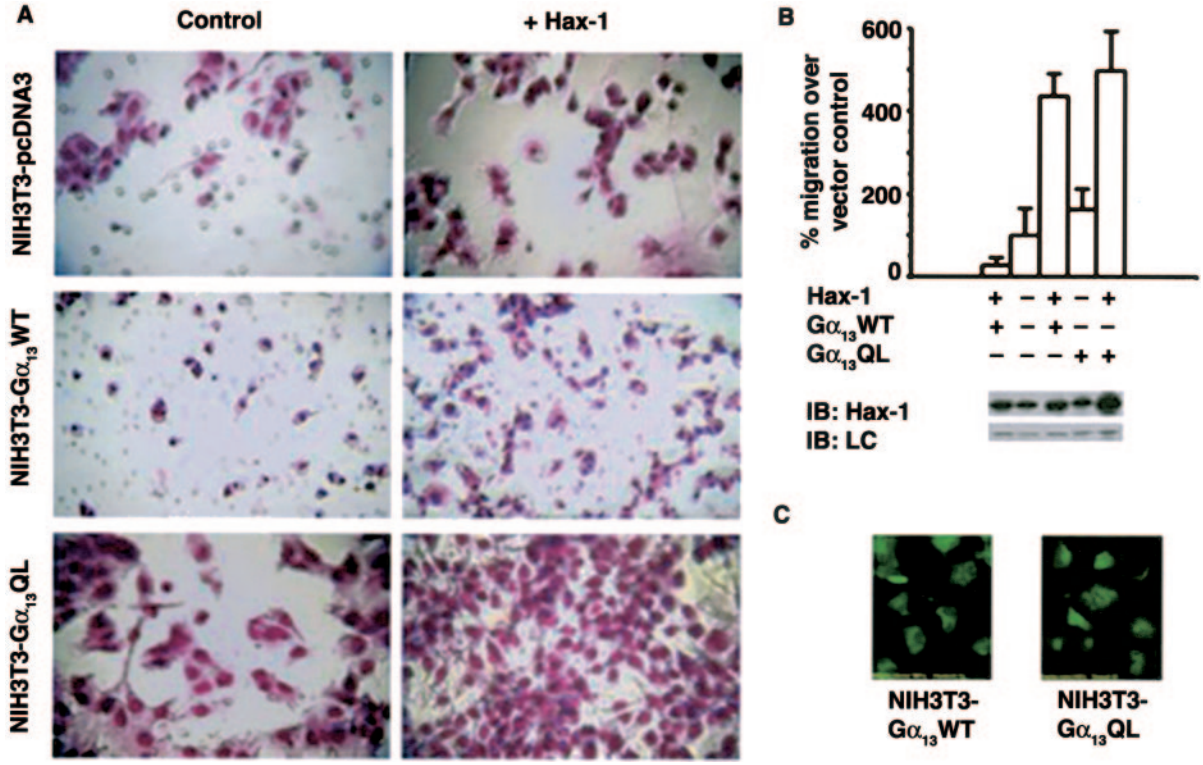

FIG. 5. **Simulation of $G\alpha_{13}$-mediated cell migration by Hax-1.** *A*, $G\alpha_{13}$-mediated cell motility is potentiated by Hax-1. NIH3T3 cells stably expressing empty vector (*NIH3T3-pcDNA3*), $G\alpha_{13}$QL (*NIH3T3-Gα_{13}QL*), or $G\alpha_{13}$WT (*NIH3T3-Gα_{13}WT*) were co-transfected with 10 μg of pcDNA3-Hax-1 cDNA. At 48 h following transfection, cell migration assays were carried out with the transfectants as described under "Experimental Procedures." The experiment was repeated four times with similar results. Migration of NIH3T3-pcDNA3 cells (*top panel*), NIH3T3-$G\alpha_{13}$WT cells (*middle panel*), and NIH3T3-$G\alpha_{13}$QL cells (*bottom panel*) with (+*Hax-1*) or without the co-expression of Hax-1 (*Control*) are compared in the photomicrographs (*scale bar*, 20 μM). *B*, quantification cell motility stimulated by Hax-1. Cell migration profiles of cells transfected with pcDNA3 vector, $G\alpha_{13}$WT, or $G\alpha_{13}$QL along with Hax-1 were quantified by enumerating the migrated cells as described under "Experimental Procedures." Results are presented as % increase over the non-transfected vector control cells. *Bars* represent mean ± S.D. from four independent experiments. Immunoblots show the expression of Hax-1 in the transfectants along with the loading control, glyceraldehyde-3-phosphate dehydrogenase (*lower panel*). *C*, verification of Hax-1 transfection in migrated cells. Migration of the Hax-1 transfectants was verified by co-expressing 1 μg of pCEFL-GFP along with pcDNA3-Hax-1 (10 μg) and imaging the fluorescence of GFP in the migrated cells.

$G\alpha_{13}$ stimulates the formation of focal adhesion complexes through the small GTPase Rho (19, 20). It has also been demonstrated that $G\alpha_{13}$ stimulates signaling pathways regulated by the small GTPase Rac (17). Whereas Rho-stimulated stress fiber and focal adhesion complex formations are often associated with cell adhesion, Rac-stimulated membrane ruffling and lamellipodia formation are associated with cell protrusion during cell movement (21, 22). Although these two responses seem to contradict each other, cell migration often involves a sequential as well as spatio-temporal regulation of adhesion, de-adhesion, and protrusion mechanisms involving both of these GTPases (3, 4). Therefore, it is possible that $G\alpha_{13}$ can transmit adhesion and protrusion signals to the actin cytoskeleton by recruiting different signaling components in a context-specific manner. If such a differential signaling for cell movement is promoted by $G\alpha_{13}$-Hax-1 interaction, a decrease in stress fiber formation with a concomitant increase in actin-rich structures at the leading edges of the cell, a characteristic feature of cell migration, should be observed. This was investigated by analyzing the actin organization in cells expressing $G\alpha_{13}$QL and Hax-1 (Fig. 3). Consistent with previous findings (19, 20), actin staining showed that NIH3T3 cells expressing $G\alpha_{13}$QL as well as the control group showed extensive stress fiber formations. However, upon expression of Hax-1, cells expressing $G\alpha_{13}$QL showed a drastic reduction in the number of stress fibers along with the formation of actin-rich structures within the periphery of the membrane ruffles. It should be noted here that the observed actin reorganization is analogous to the one stimulated by Ras during cell migration, wherein Ras promotes Rac-mediated lamellipodia formation with a reduction in actin stress fibers so that the cells can repetitively adhere, de-adhere, and move (23).

Differential Effects of Hax-1 on $G\alpha_{13}$-mediated Activation of Rho-GTPases—Because stress fiber formation has been shown to be directly correlated with Rho activity (19, 20) and the co-expression of $G\alpha_{13}$QL and Hax1 showed a reduction in stress fiber formation (Fig. 3), we sought to investigate whether the co-expression of Hax-1 would suppress $G\alpha_{13}$QL-mediated Rho activation. Whereas the expression of $G\alpha_{13}$QL stimulated Rho activity confirming previous results (19, 20, 24, 25), co-expression of Hax-1 drastically attenuated the Rho activity stimulated by $G\alpha_{13}$QL (Fig. 4*A*). Although, the mechanism(s) through which Hax-1 inhibits Rho activity remains to be resolved, it is possible that Hax-1 sequesters $G\alpha_{13}$ thereby preventing it from interacting with the Rho-guanine-nucleotide exchange factor in stimulating Rho. Based on the formation of actin-rich structures in these cells, often associated with Rac (26), it can be deduced that the co-expression of Hax-1 would potentiate $G\alpha_{13}$QL-mediated Rac activation. To test this postulate, we investigated whether the coexpression of Hax-1 modulated any changes in $G\alpha_{13}$QL-stimulated Rac activity.

In contrast to its effect on Rho activity, Hax-1 potentiated $G\alpha_{13}$QL-stimulated Rac activity in these cells. An analysis of Rac activity indicated that while Rac is stimulated by the expression of $G\alpha_{13}$QL in NIH3T3 cells (Fig. 4*B*), coexpression of Hax further enhanced such $G\alpha_{13}$QL-stimulated Rac activity. Thus, the co-expression of Hax-1 appears to differentially modulate the ability of $G\alpha_{13}$ to stimulate Rho and Rac. Although

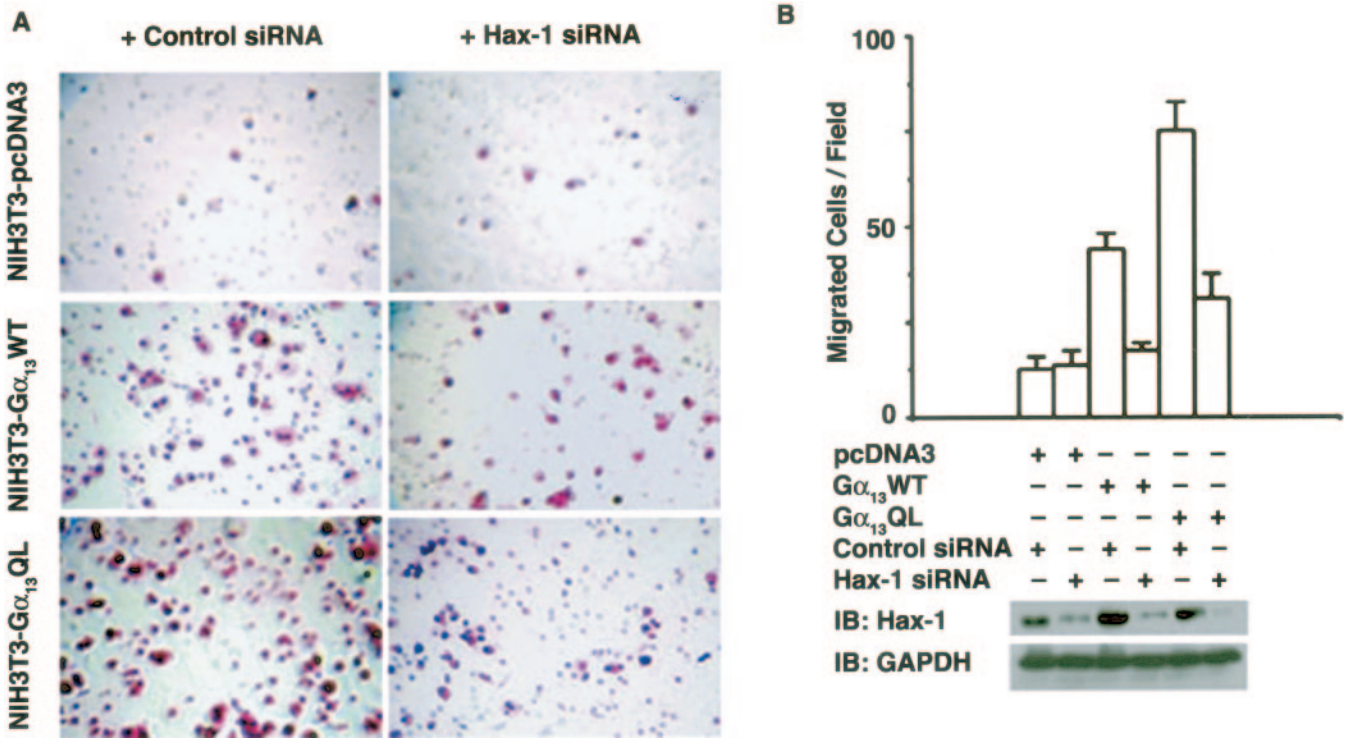

FIG. 6. **Effect of silencing Hax-1 on $G\alpha_{13}$-mediated cell migration.** *A*, inhibition of $G\alpha_{13}$-mediated cell motility by siRNA to Hax-1. Micrographs showing the inhibition of cell migration by silencing endogenous Hax-1 in NIH3T3 cells stably expressing pcDNA3, $G\alpha_{13}$WT, and $G\alpha_{13}$QL were transfected with control nonspecific siRNA duplexes or siRNA (*Control siRNA*) targeted at Hax-1 (*Hax-1 siRNA*). The migration assay was carried out against 5% serum with appropriate controls. Migration of NIH3T3 cells expressing empty vector (NIH3T3-pcDNA3, *top panel*), $G\alpha_{13}$WT (NIH3T3-$G\alpha_{13}$WT, *middle panel*), and $G\alpha_{13}$QL (NIH3T3-$G\alpha_{13}$QL, *bottom panel*) in which the expression of Hax-1 was silenced (+*Hax-1 siRNA*) were compared with those that expressed control siRNA (+*control siRNA*). *B*, quantification of Hax-1 siRNA-mediated inhibition. Cell migration profiles were quantified by enumerating the migrated cells in a minimum of three fields. Results are expressed as number of cells migrated per field and *bars* represent the mean from four independent experiments (mean ± S.D.). Silencing of endogenous Hax-1 by Hax-1-siRNA was monitored by Hax-1 immunoblot analysis (*lower panel*). *GAPDH*, glyceraldehyde-3-phosphate dehydrogenase.

the mechanism(s) through which Hax-1 potentiates $G\alpha_{13}$-mediated Rac activation remains unknown, the finding that Hax-1 enhances $G\alpha_{13}$ stimulation of Rac is of great physiological significance in the context of cell movement regulated by $G\alpha_{13}$. Because it has been shown that activated Rac is involved in translocating cortactin to membrane ruffles where cortactin stimulates actin-related protein 2/3-mediated actin polymerization (10–13), we investigated the possibility that $G\alpha_{13}$-Hax-1 interaction plays a critical role in Rac-mediated translocation of cortactin and subsequent membrane ruffling. Because the actin-rich membrane ruffling precedes the formation of cell protrusion *en route* to cell migration, these findings suggest that $G\alpha_{13}$ and Hax-1 promote the critical actin cytoskeletal reorganization necessary for cell migration.

Role of Hax-1 in $G\alpha_{13}$-mediated Cell Movement—To investigate the role of Hax-1 in $G\alpha_{13}$-mediated cell migration, Hax-1 was transiently expressed in NIH3T3 cells stably expressing $G\alpha_{13}$QL. When these cells were analyzed for migration, the results indicated that Hax-1 increased the migration of $G\alpha_{13}$QL-NIH3T3 cells by 3-fold (Fig. 5, *A* and *B*). Because lysophosphatidic acid and lysophosphatidic acid-like agonists in the serum can activate wild-type $G\alpha_{13}$ ($G\alpha_{13}$WT) through their cognate receptors (26), we tested whether Hax-1 promotes receptor-stimulated migration of NIH3T3-$G\alpha_{13}$WT toward 5% serum. The results clearly demonstrated that Hax-1 increased the migration of these cells over the vector controls by 2.5-fold (Fig. 5, *A* and *B*). Expression of Hax-1 in migrated cells was verified by monitoring the fluorescence of the co-transfected pCEFL-GFP in NIH3T3-$G\alpha_{13}$WT and NIH3T3-$G\alpha_{13}$QL cells (Fig. 5*C*).

Further analysis was carried out to test the effects of inhibiting Hax-1 on $G\alpha_{13}$-mediated cell migration. siRNAs specific to Hax-1 or nonspecific control siRNAs were transfected into NIH3T3-$G\alpha_{13}$WT cells and the migrations of these transfectants toward 5% serum were analyzed. Silencing of the endogenous Hax-1 by Hax-1-siRNA reduced the migration of NIH3T3-$G\alpha_{13}$WT cells (Fig. 6*A*), whereas there was no effect with control siRNA. Similar results were obtained with NIH3T3-$G\alpha_{13}$QL cells in which Hax-1 was silenced by siRNA (Fig. 6*A*). Quantification of these results indicated that Hax-1 siRNA reduced migration of NIH3T3-$G\alpha_{13}$WT as well as NIH3T3-$G\alpha_{13}$QL cells by 60% (Fig. 6*B*). The extent of reduction in cell migration upon silencing Hax-1 can be correlated with the siRNA-mediated reduction in the Hax-1 expression levels (Fig. 6*B*, *lower panel*). Quantification of the immunoblots showed that Hax-1 protein expression was reduced to 50–65% by 96 h after transfection. These results strongly indicate that Hax-1 plays a critical role in $G\alpha_{13}$-mediated cell migration.

Quadnary Complex Consisting of $G\alpha_{13}$, Hax-1, Cortactin, and Rac—In this context, it should be noted that cortactin, the previously known binding partner of Hax-1 is critically involved in actin polymerization and cell movement (10–13). Whereas it has been shown that the cortactin/HS1 interacting site of Hax-1 is located around amino acid 114 (14), the core domain of Hax-1 involved in $G\alpha_{13}$ interaction spans a region encompassing amino acids 176–247 (Fig. 1). As the Hax-1 domains involved in cortactin interaction and $G\alpha_{13}$ interactions are non-overlapping, it can be envisioned that Hax-1 interacts with both $G\alpha_{13}$ and cortactin in promoting cell movement. Thus, Hax-1, through its interaction with cortactin on the one hand and $G\alpha_{13}$ with the other, is likely to be involved in tethering $G\alpha_{13}$ to the membrane-ruffling site, which is involved in the formation of cell protrusion. In such an

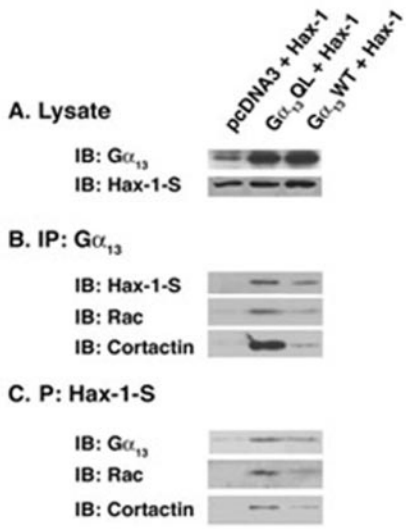

FIG. 7. **$G\alpha_{13}$ and Hax-1 are in quadnary complex containing cortactin and Rac.** *A*, co-expression of $G\alpha_{13}$ and Hax-1 in COS-7 cells. COS-7 cells were cotransfected with pcDNA3 constructs encoding S-epitope-tagged Hax-1 along with $G\alpha_{13}$WT (Hax-1 + $G\alpha_{13}$WT), or $G\alpha_{13}$QL (Hax-1 + $G\alpha_{13}$QL) in addition to vector control (pcDNA3 + Hax-1). Expression of the transfected $G\alpha_{13}$WT, $G\alpha_{13}$QL, and Hax-1 were monitored by immunoblot (*IB*) analyses of the cell lysates (*panel A* under *Lysates*). *B*, co-immunoprecipitation (*IP*) with $G\alpha_{13}$ antibodies. $G\alpha_{13}$ was immunoprecipitated from the lysates using to $G\alpha_{13}$ (*IP*, *$G\alpha_{13}$*). The immunoprecipitates were resolved by SDS-PAGE, transferred onto polyvinylidene difluoride membrane, and subjected to immunoblot analysis with antibodies to Hax-1 (*IB*: *Hax-1*) followed by successive stripping and probing with antibodies to Rac (*IB*: *Rac*) and cortactin (*IB*: *Cortactin*), respectively. *C*, co-precipitation with S-protein-agarose. S-epitope-tagged Hax-1 was precipitated from the lysates using S-protein-agarose (*P: Hax-1-S*). The immunoprecipitates were resolved by SDS-PAGE, transferred onto polyvinylidene difluoride membrane, and subjected to immunoblot analysis with antibodies to $G\alpha_{13}$ (*IB*, *$G\alpha_{13}$*). The blots were stripped and reprobed with antibodies to Rac (*IB*, *Rac*) and cortactin (*IB*, *Cortactin*) respectively.

event, Hax-1 would form a physical complex involving both $G\alpha_{13}$ and cortactin.

To investigate the presence of such complex, COS-7 cells were transfected with either S-epitope-tagged Hax-1 and $G\alpha_{13}$QL (Fig. 7*A*). Examination of S-tagged Hax-1 precipitates for the presence of $G\alpha_{13}$ and cortactin indicated that $G\alpha_{13}$ and cortactin were coimmunoprecipitated with Hax-1 (Fig. 7*B*). Likewise, the analyses of $G\alpha_{13}$ immunoprecipitates for the presence of Hax-1 and cortactin indicated that Hax-1 and cortactin were coimmunoprecipitated along with $G\alpha_{13}$ (Fig. 7*C*). Because Rac, unlike Rho, is involved in the translocation of cortactin (13) and Rac activity is enhanced in $G\alpha_{13}$-Hax-1 cotransfectants, we also examined the presence of Rac in these immunoprecipitates. Results indicated that Rac was coimmunoprecipitated along with $G\alpha_{13}$ as well as Hax-1 (Fig. 7, *B* and *C*). Together these results indicate the presence of a quadnary complex involving $G\alpha_{13}$, Hax-1, cortactin, and Rac. In light of the critical roles played by Rac and cortactin in cell protrusion and migration, it can be inferred that Hax-1 association with $G\alpha_{13}$ brings them closer to the active site of cell protrusion, where the stimulation of Rac activity by $G\alpha_{13}$ would have a more pronounced effect on cell movement.

DISCUSSION

Considering the observations that 1) $G\alpha_{13}$ stimulates the activation of Rac, which is potentiated by Hax-1 (Fig. 4); 2) Rac stimulates the translocation of cortactin (10, 13); 3) cortactin stimulates actin polymerization leading to lamellipodia formation (11–13); 4) Hax-1 promotes $G\alpha_{13}$-mediated cell motility (Figs. 5 and 6); and 5) $G\alpha_{13}$ is in complex with Hax-1, cortactin, and Rac (Fig. 7), it is reasonable to conclude that both $G\alpha_{13}$ and Hax-1 are part of a signaling complex involved in cell motility. It is likely that such proximal positioning of $G\alpha_{13}$, Rac, Hax-1, and cortactin stimulates cell migration by countering $G\alpha_{13}$-Rho-mediated cell adhesion (Fig. 8). The studies presented here demonstrate for the first time a novel interaction between $G\alpha_{13}$ and the cytoskeleton-associated protein Hax-1, thereby identifying a cytoskeletal signaling locus for $G\alpha_{13}$ in cell movement.

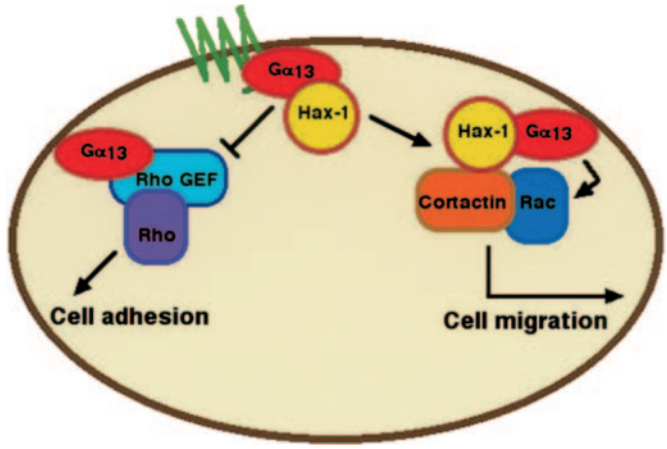

FIG. 8. **Proposed model for $G\alpha_{13}$-Hax-1-mediated regulation of cell motility.** Association of Hax-1 with $G\alpha_{13}$ leads to a reduction in $G\alpha_{13}$-mediated activation of Rho along with a concomitant increase in $G\alpha_{13}$-mediated activation of Rac. By tethering $G\alpha_{13}$ to cortactin in a complex containing Rac, Hax-1 brings $G\alpha_{13}$ closer to cortactin, which in turn can be stimulated by $G\alpha_{13}$-activated Rac, to initiate actin polymerization, cell protrusion, and subsequent cell movement.

Based on the results, it can be envisioned that Hax-1 plays a central role in $G\alpha_{13}$-mediated cell motility by affecting three distinct, but closely related, signaling loci. First, by associating with $G\alpha_{13}$, Hax-1 sequesters $G\alpha_{13}$ from activating Rho and associated cell adhesion pathways. Second, through the potentiation of $G\alpha_{13}$-stimulated Rac activity, Hax-1 promotes Rac-mediated translocation of cortactin to the periphery where cortactin along with actin-related proteins induces cell protrusion and migration. Finally, by tethering $G\alpha_{13}$ to cortactin in a complex containing Rac, Hax-1 provides a signaling nexus that facilitates the dynamic and uninterrupted transmission of signals from $G\alpha_{13}$ to cortactin through Rac to promote cell protrusion and migration.

Our present study does not address the mechanism(s) through which Hax-1 potentiates $G\alpha_{13}$-mediated Rac activation. However, it is interesting to note that Hax-1 contains the characteristic P*XXX*P motif (amino acids 198–202, P*XXX*P motif flanked by P*XX*P motifs on either side), which is known to be the binding motif for the PIX family of Rac/CDC42 guanine-nucleotide exchange factors (27). Therefore, it is possible that Hax-1 potentiates Rac activation by bringing $G\alpha_{13}$ closer to a specific Rac-guanine-nucleotide exchange factor. Although our initial studies did not identify such interaction between PIX-β and Hax-1,[2] it is possible that a closely related guanine-nucleotide exchange factor may interact with Hax-1 through this site or other P*XX*P sites that are present in Hax-1. Further studies should define the mechanisms through which Hax-1 potentiates $G\alpha_{13}$-stimulated activation of Rac.

Previous studies have shown that $G\alpha_{13}$ is critically required for the development of mouse embryos as $G\alpha_{13}-/-$ embryos are resorbed by day 10.5 (8). The lethality of the $G\alpha_{13}-/-$ genotype is ascribed to the loss of $G\alpha_{13}$-mediated cell motility associated with embryonic angiogenesis. It is intriguing to note that $G\alpha_{12}$,

[2] J. H. Ha and N. Dhanasekaran, unpublished data.

although it shares 67% amino acid identity with $G\alpha_{13}$ (6), failed to compensate for the loss of $G\alpha_{13}$ in these embryos. Because both $G\alpha_{12}$ and $G\alpha_{13}$ can be stimulated by the same receptors to activate similar cellular responses, the molecular basis for the differential effect on cell motility remained elusive. In this context, the results presented here demonstrate that Hax-1 specifically interacts with $G\alpha_{13}$ but not $G\alpha_{12}$, and that such interaction is critical for $G\alpha_{13}$-mediated cell motility that provides a molecular basis for such unique and differential signaling by $G\alpha_{13}$. Further studies should define the role of $G\alpha_{13}$-Hax-1 complexes in physiological responses that require cell movement or cytoskeletal changes mediated by $G\alpha_{13}$. In light of the recent findings that Hax-1 is differentially expressed in hypoxic tumor progression (28) and overexpressed in many different metastatic tumors as indicated by SAGE analysis (28–30), it is more likely that $G\alpha_{13}$-Hax-1 interaction plays a critical role in the metastatic phenotype of these tumors.

Acknowledgments—We are grateful to Dr. R. A. Vaillancourt for yeast strains and yeast vectors and Dr. T. Watanabe for Hax-1 full-length cDNA. Helpful discussions and critical reading of the manuscript by Rashmi Kumar and Kimia Kashef are gratefully acknowledged.

REFERENCES

1. Franz, C. M., Jones, G. E. & Ridley, A. J. (2002) *Dev. Cell* **2,** 153–158
2. Vicente-Manzanres, M., Sancho, D., Yanez-Mo, M. & Sanchez-Madrid, F. (2002) *Int. Rev. Cytol.* **216,** 233–289
3. Rodriguez, O. C., Schaefer, A. W., Mandato, C. A., Forscher, P., Bement, W. M. & Waterman-Storer, C. M. (2003) *Nat. Cell Biol.* **5,** 599–609
4. Mitchison, T. J. & Cramer, L. P. (1996) *Cell* **84,** 371–379
5. Rossi, D. & Zlotnik, A. (2000) *Annu. Rev. Immunol.* **18,** 217–242
6. Radhika, V. & Dhanasekaran, N. (2001) *Oncogene* **20,** 1607–1614
7. Parks, S. & Wieschaus, E. (1991) *Cell* **64,** 447–458
8. Offermanns, S., Mancino, V., Revel, J.-P. & Simon, M. I. (1997) *Science* **275,** 533–536
9. Gu, J. L., Muller, S., Mancino, V., Offermanns, S. & Simon, M. I. (2002) *Proc. Natl. Acad. Sci. U. S. A.*, **99,** 9352–9357
10. Patel, A. S., Schechter, G. L., Wasilenko, W. J. & Somers, K. D. (1998) *Oncogene* **16,** 3227–3232
11. Uruno, T., Liu, J., Zhang, P., Fan, Y-X., Egile, C., Li, R., Mueller, S. C. & Zhan, X. (2001) *Nat. Cell Biol.* **3,** 259–266
12. Uruno, T., Zhang, P., Liu J., Hao, J. J. & Zhan, X. (2003) *Biochem. J.* **371,** 485–493
13. Weed, S. A., Du, Y. & Parsons, J. T. (1998) *J. Cell Sci.* **111,** 2433–2443
14. Suzuki, Y., Demoliere, C., Daisuke, K., Takeshita, H., Deuschle, U. & Watanabe, T. (1997) *J. Immunol.* **158,** 2736–2744
15. Noel, J. P., Hamm, H. E. & Sigler, P. B.(1993) *Nature* **366,** 654–663
16. Gallagher, A. R., Cedzich, A., Gretz, N., Somlo, S. & Witzgall, R. (2000) *Proc. Natl. Acad. Sci. U. S. A.* **97,** 4017–4022
17. Plonk, S. G., Park, S-K. & Exton, J. H. (1998) *J. Biol. Chem.* **273,** 4823–4826
18. Yuan, J., Slice, L. W. & Rozengurt, E. (2001) *J. Biol. Chem.* **276,** 38619–38627
19. Buhl, A. M., Johnson, N. L., Dhanasekaran, N. & Johnson, G. L. (1995) *J. Biol. Chem.* **270,** 24631–24634
20. Hooley, R., Yu, C-Y., Symons, M. & Barber, D. L. (1996) *J. Biol. Chem.* **271,** 6152–6158
21. Hall, A. (1998) *Science* **279,** 509–514
22. Ridley, A. J. (2001) *J. Cell Sci.* **114,** 2713–2722
23. Vial, E., Sahai, E. & Marshall, C. J. (2003) *Cancer Cell* **4,** 6779
24. Kozasa, T., Jiang, X., Hart, M. J., Sterweis, P. M., Singer, W. D., Gilman, A. G., Bollag, G. & Sternweis, P. C. (1998) *Science* **280,** 2109–2111
25. Chikumi, H., Fukuhara, S. & Gutkind, J. S. (2002) *J. Biol. Chem.* **277,** 12463–12473
26. Gohla, A., Harhammer, R. & Schultz, G. (1998) *J. Biol. Chem.* **273,** 4653–4659
27. Manser, E., Loo, T. H., Koh, C. G., Zhao, Z. S., Chen, X. Q., Tan, L., Tan, I., Leung, T. & Lim, L. (1998) *Mol. Cell* **2,** 183–192
28. Jiang, Y., Zhang, W., Keichii, K., Klco, J. M., Martin, St. T. B., Dufault, M. R., Madden, S. L., Kaelin, W. G. & Nacht, M. (2003) *Mol. Cancer Res.* **1,** 453–462
29. Velculescu, V. E., Zhang, L., Vogelstein, B. & Kinzler, K. W. (1995) *Science* **270,** 484–487
30. Mirmohammadsadegh, A., Tartler, U., Michel, G., Baer, A., Walz, M., Wolf, R., Ruzicka, T. & Hengge, U. R. (2003) *J. Investig. Dermatol.* **120,** 1045–1051
31. Dermott, J. M., Ha, J. H., Lee, C. H. & Dhanasekaran, N. (2004) *Oncogene* **23,** 226–232
32. Dermott, J. M. & Dhanasekaran, N. (2002) *Methods Enzymol.* **344,** 298–309
33. Radhika, V., Naik, N. R., Advani, S. H. & Bhisey, A. N. (2000) *Cytometry* **42,** 379–386

$G\alpha_{13}$ Stimulates Cell Migration through Cortactin-interacting Protein Hax-1

V. Radhika, Djamila Onesime, Ji Hee Ha and N. Dhanasekaran

J. Biol. Chem. 2004, 279:49406-49413.
doi: 10.1074/jbc.M408836200 originally published online August 31, 2004
